Modern Applied Science; Vol. 9, No. 6; 2015
ISSN 1913-1844 E-ISSN 1913-1852
Published by Canadian Center of Science and Education

Effect of Liquid Layer Thickness on the Ablation Efficiency and the Size-Control of Silver Colloids Prepared by Pulsed Laser Ablation

Mohammed A. Al-Azawi[1], Noriah Bidin[2], Abdulrahman K. Ali[3], Khaleel I. Hassoon[3] & Mundzir Abdullah[1]

[1] Department of Physics, Faculty of Science, Universiti Teknologi Malaysia, Johor Bahru, Johor, Malaysia

[2] Advance Photonic Science Institute, Faculty of Science, Universiti Teknologi Malaysia, Johor Bahru, Johor, Malaysia

[3] Laser and Optoelectronics Branch, Department of Applied Sciences, University of Technology, Baghdad, Republic of Iraq

Correspondence: Noriah Bidin, Advance Photonic Science Institute, Faculty of Science, Universiti Teknologi Malaysia, Johor Bahru, Johor, Malaysia. E-mail: noriah@utm.my/mohammed.a.alazawi@gmail.com

Received: December 10, 2014 Accepted: December 24, 2014 Online Published: March 24, 2015

doi:10.5539/mas.v9n6p20 URL: http://dx.doi.org/10.5539/mas.v9n6p20

Abstract

Sliver colloidal solutions were synthesized by Nd: YAG laser ablation 1064 nm of a high purity silver target immersed in deionised water. The effect of water layer thickness on the laser ablation efficiency of nanoparticles was investigated experimentally. UV-Vis spectrophotometer and transmission electron microscopy observations were employed to characterize the optical spectra and particle sizes of colloids, respectively. The optimum parameter of the water layer thickness (which yielded the maximum ablation efficiency) was determined. It was demonstrated that both: the average particle size and the ablation efficiency which can be tuned by choosing suitable experimental parameters of liquid layer thickness, laser fluence and post-ablation laser wavelength. Average particle size and redistribution of nanoparticles was controlled by the subsequent treatment of the ablated colloid solution with combination of 1064 and 532 nm pulses. The effects of post-ablation under laser-induced particle modification reduced the average particle size from 15.1 to 4.3 nm. Particle size distribution was also narrowed with 532 nm pulses.

Keywords: laser ablation, silver nanoparticles, ablation efficiency, laser irradiation

1. Introduction

Nanoparticles of noble metals are the essential structures of nanotechnology and have draw much attention from researchers due to their size dependent electronic, catalytic, magnetic, and optical properties (Desarkar et al., 2012; Hajiesmaeilbaigi et al., 2006). Almost, all physical properties of the materials change significantly as the size of the constituting particles reaches the nanoscale regime. These variations in properties result from the presence of a small number of atoms in each particle and a high surface-to-volume ratio, due to the large fraction of atoms that reside on the particle's surface, as well as the electronic energy bands having control over the majority of the physical and chemical properties being drastically modified (Dorranian et al., 2013; Huang et al., 2009). The spacing of electronic levels and bandgap increases with the decreasing particle size. This is because the electron - hole pairs and the Columbic interaction between them are much closer together (Schmid, 1992; Zhang, 2003). With regards to the UV-Vis optical spectra silver colloidal; this increase in the bandgap can be observed experimentally *via* the blue-shift in the absorption spectrum. These size-dependent silver nanoparticle (Ag NPs) properties are exploited in many potential applications such as antibacterial activity (Das et al., 2011), solar energy conversion (Berginc et al., 2014), light-emitting devices (Qiao et al., 2013), chemical/biological sensors (Frederix et al., 2003; Joshi and Kruis, 2006), and photocatalysis (Linic et al., 2011).

Silver nanoparticles have an advantage over other metal nanoparticles (e.g., gold and copper) since the Surface Plasmon Resonance (SPR) energy of Ag is located far from the inter band transition energy (Hajiesmaeilbaigi, et al., 2006). Therefore, the position of SPR peak for silver nanoparticles in water can be controlled over a range of 380 – 500 nm by changing the particle size to obtain a unique property. The successful establishment of this important part of nanotechnology depends first on the control of particle size, morphology, and the composition of metal nanoparticles during synthesis. Generally, metal NPs can be prepared by various physical and chemical

methods. Pulsed Laser Ablation in Liquids (PLAiL) is currently exploited as a physical metal nanoparticles preparation method. This method is based on pulse laser ablation from bulk metals in a liquid environment (e.g., water). One advantage of this method, compared to other conventional methods for preparing metal colloids, is the simplicity of the procedure; with respect to metals or solvents that do not need a catalyst, etc. Furthermore, it is a clean method due to the absence of chemical reagents or ions in the final preparation (Liu et al., 2010). Nevertheless, the PLAiL technique lacks from the low ablation efficiency of NPs and the size distribution of the NPs synthesized by this technique tends to be broadened due to both postablation aggregation of NPs and the possible ejection of large fragments from the target surface during the ablation process (Tarasenko et al., 2006; Yang, 2012). This disadvantage significantly reduces the applicability of PLAiL in synthesizing NPs.

In solid-liquid laser ablation, the surrounding liquid influences the laser-induced breakdown at the solid–liquid interface and confines the generated plasma. The physical properties of liquid (e.g., polarity and temperature) determine the morphology, stability, and growth of the synthesized NPs (Yang, 2012). The liquid used in laser ablation converts a portion of the laser energy into mechanical impulse by vaporization and plasma generation. This impulse transfers the ablated species and induces shockwaves. In most cases, the water-phase is favourable, because it does not absorb too much light, is a cheap and safe medium and exhibits a high heat capacity (Kruusing, 2004). At short laser pulses in nanoseconds – solid interaction, the ablation process is dominated by heat conduction, melting, evaporation, and plasma formation. In order for this process to be effective, the energy of the laser pulse must be absorbed by the material (Kabashin et al., 2010; Leitz et al., 2011). Numerous studies have reported that the ablation efficiency and characteristics of silver nanoparticles depends extremely upon numerous laser parameters that include wavelength, pulse duration (in the femto-, pico- and nanosecond regimes), fluence, ablation time duration, and effective liquid medium, with or without the presence of surfactants (Hajiesmaeilbaigi, et al., 2006; Naseri et al., 2014; Tsuji et al., 2001; Tsuji et al., 2002; Tsuji et al., 2008). commonly, correlation between the ablation efficiency and thickness of the surrounding liquid layer has not yet been carried out (or mentioned) by many researchers before.

In this work, we endeavour to optimize the ablation efficiency of Ag NPs synthesized by laser ablation of the metal plate in deionised water, without adding any chemical materials. This study was addressed practically by investigating the effect of the liquid layer thickness above the target. At sufficiently high laser fluence, we attempted to identify the experimental conditions of these parameters that played an important role in the formation of a large amount of NPs. Meanwhile, the influence of post-ablation manipulation under laser-induced modification, on both the ablation efficiency and the final particle size of the ablated metallic colloidal solution, was discussed.

2. Experimental Methods

A highly pure Ag plate (purity, > 99.999%) with a thickness of 2 mm and surface area of 25×25 mm^2 was employed for this research as the target material. The plate surface was initially treated with emery paper sheet (with a 500 grit size) to remove surface imperfections. The plate was then cleaned with ethanol, placed with an ablation vessel in an ultrasonic bath, and rinsed with deionized water before each experiment, in order to eliminate any contaminants present. The target was kept at the bottom of a Pyrex vessel (volume, 15 mL) filled with ultrapure 18.2 MΩ deionised water as a layer (with a thickness of 10–18 mm above the surface). A pulsed Nd:YAG laser (fundamental wavelength, 1064 nm; pulse duration, 8 ns; repetition rate, 1 Hz) was employed as an irradiation source during ablation. Experiments were conducted by adjusting the laser beam (fluence, 15 J/cm^2) and focusing on the target surface through a converging lens (focal length, 10 cm) for 4 mins at room temperature. During ablation, the Ag colloidal solution was magnetically stirred to remove the Ag NPs from the laser's path.

The optical spectra of these colloidal solutions were characterized with a UV-Vis spectrophotometer (Perkins-Elmer, Lambda 25). A quartz cuvette (path length, 0.5 cm) was used to measure the absorption. A transmission electron microscope (TEM; Philips CM12; accelerating voltage, 120 kV) was used to obtain the micrographs of the Ag NPs. The Ag colloidal solution was placed in the ultrasonic bath for 20 min.. A small drop of the sample solution was then placed onto the carbon-coated copper grid and dried at room temperature. The size distribution of each sample was obtained by counting at least 250 particles in the TEM image.

3. Results and Discussion

3.1 Effects of the Liquid Layer Thickness

The effects of the water layer thickness above the target surface on ablation efficiency were investigated. Figure 1a shows the typical UV-Vis optical spectra of the colloidal solution produced by ablating the Ag target at various water layer thicknesses. The absorbance of silver colloids demonstrated the characteristic features of the

Surface Plasmon Resonance (SPR). The absorption spectra of colloidal suspensions consisted of a strong absorption (around 398- 413 nm) and a weak absorption (in the 200-250 nm region) due to the plasmon transitions and the interband transitions of the Ag particles, respectively. The prominent single peaks indicate that the morphologies of the obtained Ag NPs were nearly spherical in the colloidal solution. These were also verified by the TEM results. The position and width of the SPR peak depends strongly on the Ag particle size and shape (Tolaymat et al., 2010). Therefore, the ablation efficiency was estimated from the absorbance of the interband transition at 250 nm; because this absorbance does not shift with the particle size, but is sensitive to the number of particles (Tarasenko, et al., 2006). As shown in Figure 1a, this efficiency and the position of the SPR peak was found to be dependent on the thickness of the water layer above the target' surface. The position of the SPR peak at a layer thickness of 14 mm was slightly shifted towards a shorter wavelength; thus indicating a certain decreasing of particle size (Nakamura et al., 2013). Figure 1b demonstrates the absorbance of the interband transitions of the Ag colloidal solution at 250 nm, based on small changes in the water layer thickness. As the thickness of the water layer increased the ablation efficiency increased linearly, until it reached its maximum value of 14 mm; above this value, the ablation efficiency decreased rapidly with any further thickness increase. This result was attributed to the increase in the properties of the plasma (e.g., temperature, pressure, and density) caused by its layer confinement. The confined plasma plume adiabatically expanded within a certain layer thickness. The energy concentrated in this plasma increased on the target surface, resulting in more efficient of ablation. However, the layer thickness of above 14 mm enhanced the solution absorption of laser energy. A small portion of the energy reached the target's surface which causes a decrease in the quantity of ablated species, thereby decreasing the ablation efficiency. Thus, the effects of both the plasma plume and the water layer thickness on nanoparticle production during ablation process should be equal, in order to optimize the ablation efficiency. These results suggested that the optimum value of water layer thickness was 14 mm.

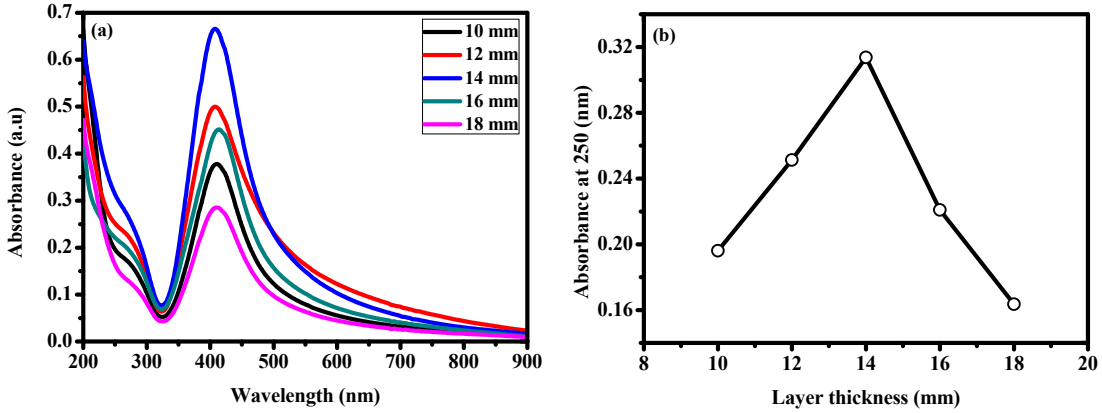

Figure 1. (a) Absorbance spectra of silver colloidal solution prepared at various thicknesses of water layers and laser fluence of 15 J/ cm^2; (b) the absorbance of the interband transitions as a function of thickness of water layer

Finally, it should be mentioned that our results at layer thickness (> 14 mm) are in good agreement with a previous observation by Kang and Welch (Kang and Welch, 2007), who reported that ablation efficiency decreased with increase of water layer thickness. However, our results contrast their results at layer thicknesses of <14 mm. They quantitatively estimated the ablation efficiency by measuring the volume of craters formed on the polymethyl-methacrylate surface in the presence of various thinner water layers at a laser pulse duration of 30 ns and 275 μs. The variance in our results over theirs must have occurred from different estimation methods used for ablation efficiency, target material, and laser beam properties. The efficiency of photon–matter interaction depends on material and laser beam properties (Kabashin, et al., 2010). In addition, the amount of material removal for a target in water, measured by crater volume, increases as the laser pulse duration decreases (Sakka et al., 2009).

3.2 Size Modification by Laser Irradiation

After the laser stopped, ablated species such as atoms, clusters and small fragments are aggregated and the size distribution of NPs tends to be broadened. To avoid this problem, the final size of these particles in the ablated colloidal solution was controlled by postablated laser-induced particle modification. The Ag plate was removed from the ablated vessel; a two-step process was immediately performed by irradiating the colloidal solution. The first step was performed using unfocused laser pulses at 1064 nm and maximum laser fluence of 1.1 J/cm^2

for five minutes. The second step was performed using unfocused laser pulses at 532 nm and maximum laser fluence of 0.7 J/cm^2 for five minutes. The colloidal solution was slowly rotated without ripples during laser irradiation Figure 2 shows the UV-Vis optical spectra of the Ag colloidal solution, which was inspected after ablation and the modification process. The Ag plate was ablated using a 1064 nm laser under optimum conditions (i.e., thickness of water layer, 14 mm; laser fluence, 15 J/cm^2) to generate the colloid solution with optical spectral characteristics via the position of the SPR peak at 409 nm. The absorbance increased considerably at interband transition after laser irradiation; indicating that the total concentration of the Ag NPs had increased in the solution. Laser irradiation, with the 1064 nm pulses on the colloidal solution, enhanced the ablation efficiency. However, the position of the SPR peak shifted slightly towards shorter wavelengths. The subsequent irradiation with the 532 nm pulses caused higher ablation efficiency than that of the 1064 nm laser. In addition, the position of the SPR peak shifted to short wavelengths from 405 to 398 nm; thus indicating that the particle size had decreased. This could be explained by the photon energy being easily transformed to the internal modes of the initial particles as heating, melting, and evaporation occurring during the interactions between the laser light and the silver particles in the colloidal solution; thus resulting in laser-induced NP modification (Tarasenko, et al., 2006). Photon-particle interaction is a powerful influence and yields an SPR excitation of the initial particles in the colloidal solution, when the incident laser wavelength falls within the absorption spectra of colloidal suspension. Therefore, irradiation by the 532 nm laser influenced the majority of NPs at the plasmon transitions of Ag colloids and yielded their size redistribution. In contrast, the irradiation by the 1064 nm laser only influenced the large sized NPs that exhibited high near-infrared region at the absorption spectra of colloidal suspensions. As the photon energy of 532 nm was higher than that of 1064 nm, so the average particle size of the Ag colloids, irradiated by 532 nm, was smaller than those irradiated by 1064 nm. The morphologies and the particle size distribution of Ag colloids were also verified by the TEM results (as discussed below). Figures 3- 5 illustrate the TEM images of the Ag NPs generated by the laser ablated Ag plate, as well as after the consecutive irradiation of the Ag colloidal solution with 1064 and 532 nm pulses. Each TEM image is accompanied by the histograms of the particle size distribution. The TEM images indicate that the majority of the NPs were spherical. As shown in Figure 3a and b, the NPs synthesized by ablation of the Ag target possessed some chains of accreted particles, with an average particle size of 15.1 nm, based on the histograms. Figures 4 and 5 suggest that the particle size distribution and average particle size of colloids were modified after consecutive irradiations by the 1064 and 532 nm lasers. The average particle size was 10.4 nm in the case of irradiation by 1064 nm laser (Figure 4); however, the size distribution of NPs became lower homogeneously, compared to that of the distribution shown in Figure 3b. Irradiation by 1064 nm may fragment the particles in relatively varying sizes at near-infrared region in the absorption spectra; thus making the width of the size distribution slightly changed. In contrast, the average particle size was 4.3 nm for the subsequent irradiation with the 532 nm laser. Furthermore, the particles were diffused with no noticeable aggregation, and the particle size distribution was narrower (Figures 5a and b). The results obtained by an analysis of the particle size distribution for each histogram are summarized in Table 1. These results included smaller average size of formed particle (< 5 nm) with a narrower size distribution compared with that reported by Tsuji et al. (Tsuji, et al., 2002), Tarasenko et. (N. Tarasenko et al., 2005), Hajiesmaeilbaigi et al. (Hajiesmaeilbaigi, et al., 2006). The difference of our results from their results can be attributed to the optimization in the experimental parameter used in our work during laser-induced particles modification process, one of them was liquid layer thickness.

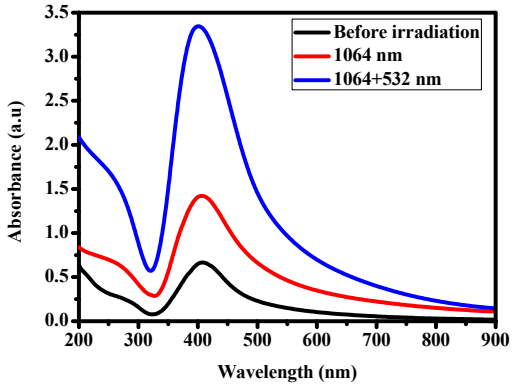

Figure 2. Absorbance spectra of the ablated silver colloidal solution at 14 mm thickness of water layer before and after the laser irradiation process. Each of the first and second steps of the laser irradiation process were carried out for 5 mins by 1064 nm laser pulses with laser fluence of 1.1 J/cm^2 and subsequent treatment by 532 nm pulses with a laser fluence of 0.7 J/cm^2

(a) (b)

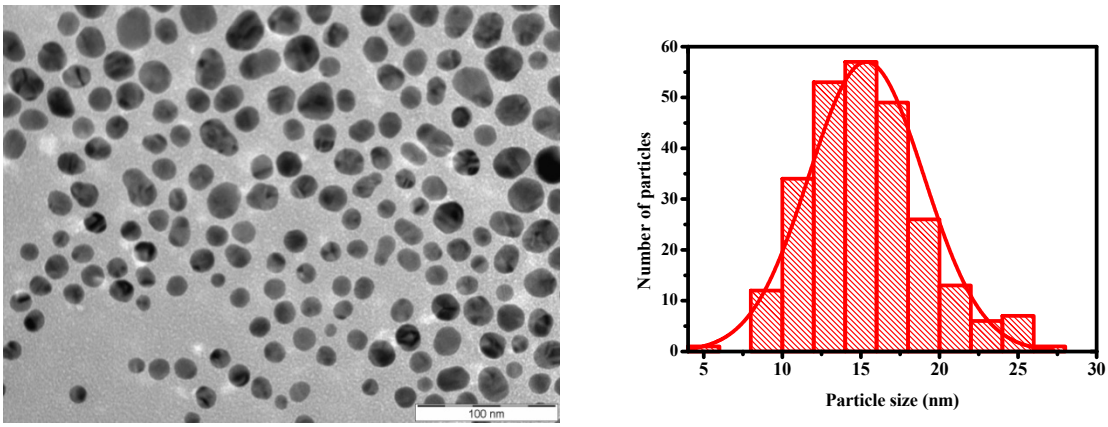

Figure 3. (a) TEM micrograph and (b) histogram of the silver nanoparticles produced by laser ablation of silver target in 14 mm thickness of deionised water at 1064 nm laser pulses and 15 J/cm^2 laser fluence for 4 mins

(a) (b)

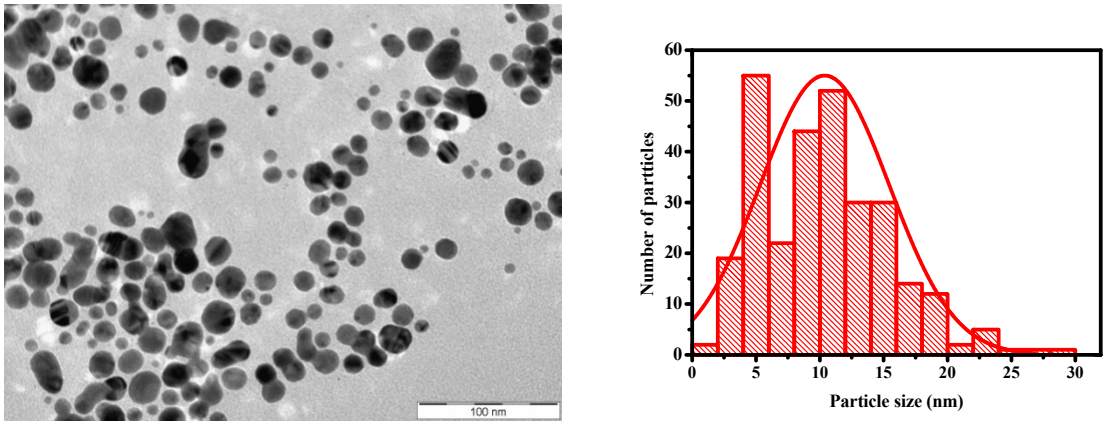

Figure 4. (a) TEM micrograph and (b) histogram of the silver nanoparticles produced after laser irradiation of the ablated colloidal solution at (1064 nm, 1.1 J/cm^2) for 5 mins

(a) (b)

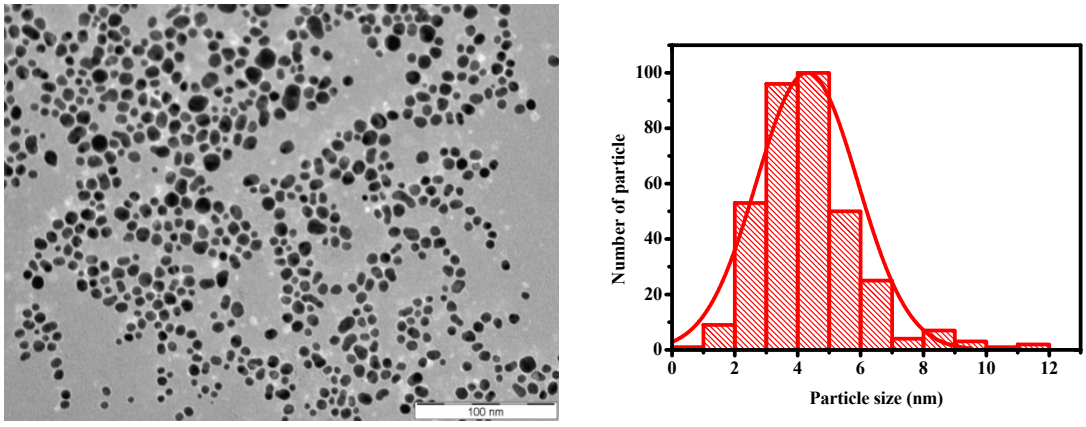

Figure 5. (a) TEM micrograph and (b) histogram of the silver nanoparticles produced after subsequent laser irradiation of the ablated colloidal solution with (532 nm, 0.7 J/cm^2) for 5 mins

Table 1. The average particle size and standard deviation of silver nanoparticles in the ablated colloidal solution before laser irradiation and after modification process

Stage	Average particle size (nm)	Standard deviation (nm)
Before irradiation	15.1	3.5
After irradiation with 1064 nm	10.4	5.1
After subsequent irradiation with 532 nm	4.3	1.6

4. Conclusion

The Ag NPs, with average particle sizes from 15.1 to 4.3 nm, were synthesized by laser ablation of an Ag target in deionised water. The laser ablation efficiency at a relatively high laser fluence of 15 J/cm^2 increased linearly with an increasing water layer thickness, until reaching its maximum value of 14 mm thickness. Subsequently, the ablation efficiency rapidly decreased with any increasing thickness. In the course of this study, the optimal water layer thickness for maximum ablation efficiency and evolution particle sizes in ablated colloidal solution was found to be equal to 14 mm. The production yield and size distribution of the ablated particles were controlled by postablated laser-induced particles modification with 1064 and 532 nm laser irradiation, without chemical additives. The results obtained showed that a high ablation efficiency of Ag NPs and small average particle size with narrow size distribution can be carried out by a compatible selection of the experimental parameters, such as water layer thickness, laser fluence, and post-ablation laser wavelength combinations. This study may be useful for synthesizing a desired quantity and size of nanoparticles in colloidal solution.

Acknowledgment

We like to express our thanks to the government of Malaysia through RUG- Flagship vote 00G79 and UTM through RMC for the financial support of this project as well as monitoring the progress of the works.

References

Berginc, M., Opara Krašovec, U., & Topič, M. (2014). Solution Processed Silver Nanoparticles in Dye-Sensitized Solar Cells. *Journal of Nanomaterials,* 2014. http://dx.doi.org/10.1155/2014/357979

Das, R., Gang, S., & Nath, S. S. (2011). Preparation and antibacterial activity of silver nanoparticles. *Journal of Biomaterials and nanobiotechnology, 2*, 472. http://dx.doi.org/10.4236/jbnb.2011.24057

Desarkar, H., Kumbhakar, P., & Mitra, A. (2012). Effect of ablation time and laser fluence on the optical properties of copper nano colloids prepared by laser ablation technique. *Applied Nanoscience, 2*(3), 285-291. http://dx.doi.org/10.1007/s13204-012-0106-8

Dorranian, D., Tajmir, S., & Khazanehfar, F. (2013). Effect of Laser Fluence on the Characteristics of Ag Nanoparticles Produced by Laser Ablation. *Soft Nanoscience Letters, 3*, 93. http://dx.doi.org/10.4236/snl.2013.34017

Frederix, F., Friedt, J.-M., Choi, K.-H., Laureyn, W., Campitelli, A., & Mondelaers, D., et al. (2003). Biosensing based on light absorption of nanoscaled gold and silver particles. *Analytical Chemistry, 75*(24), 6894-6900. http://dx.doi.org/10.1021/ac0346609

Hajiesmaeilbaigi, F., Mohammadalipour, A., Sabbaghzadeh, J., Hoseinkhani, S., & Fallah, H. (2006). Preparation of silver nanoparticles by laser ablation and fragmentation in pure water. *Laser Physics Letters, 3*(5), 252. http://dx.doi.org/10.1002/lapl.200510082

Huang, X., Neretina, S., & El Sayed, M. A. (2009). Gold nanorods: from synthesis and properties to biological and biomedical applications. *Advanced Materials, 21*(48), 4880-4910. http://dx.doi.org/10.1002/adma.200802789

Joshi, R. K., & Kruis, F. E. (2006). Influence of Ag particle size on ethanol sensing of SnO 1.8: Ag nanoparticle films: a method to develop parts per billion level gas sensors. *Applied physics letters, 89*(15), 153116-153116-153113. http://dx.doi.org/10.1063/1.2360245

Kabashin, A., Delaporte, P., Pereira, A., Grojo, D., Torres, R., & Sarnet, T., et al. (2010). Nanofabrication with pulsed lasers. *Nanoscale research letters, 5*(3), 454-463. http://dx.doi.org/10.1007/s11671-010-9543-z

Kang, H. W., & Welch, A. J. (2007). Effect of liquid thickness on laser ablation efficiency. *Journal of Applied Physics, 101*(8), 083101-083101-083104. http://dx.doi.org/10.1063/1.2715746

Kruusing, A. (2004). Underwater and water-assisted laser processing: Part 1—general features, steam cleaning

and shock processing. *Optics and Lasers in Engineering, 41*(2), 307-327. http://dx.doi.org/10.1016/S0143-8166(02)00142-2

Leitz, K. H., Redlingshöfer, B., Reg, Y., Otto, A., & Schmidt, M. (2011). Metal ablation with short and ultrashort laser pulses. *Physics Procedia, 12*, 230-238. http://dx.doi.org/10.1016/j.phpro.2011.03.128

Linic, S., Christopher, P., & Ingram, D. B. (2011). Plasmonic-metal nanostructures for efficient conversion of solar to chemical energy. *Nature materials, 10*(12), 911-921. http://dx.doi.org/10.1038/nmat3151

Liu, P., Cui, H., Wang, C., & Yang, G. (2010). From nanocrystal synthesis to functional nanostructure fabrication: laser ablation in liquid. *Physical Chemistry Chemical Physics, 12*(16), 3942-3952. http://dx.doi.org/10.1039/b918759f

Nakamura, T., Herbani, Y., Ursescu, D., Banici, R., Dabu, R. V., & Sato, S. (2013). Spectroscopic study of gold nanoparticle formation through high intensity laser irradiation of solution. *AIP Advances, 3*(8), 082101. http://dx.doi.org/10.1063/1.4817827

Naseri, M. G., Sadrolhosseini, A. R., Dehzangi, A., Kamalianfar, A., Saion, E. B., & Zamiri, R., et al. (2014). Silver Nanoparticle Fabrication by Laser Ablation in Polyvinyl Alcohol Solutions. *Chinese Physics Letters, 31*(7), 077803. http://dx.doi.org/10.1088/0256-307X/31/7/077803

Qiao, Q., Shan, C. X., Zheng, J., Li, B. H., Zhang, Z. Z., & Shen, D. Z. (2013). Surface plasmon enhanced ultraviolet light-emitting devices. *Journal of Luminescence, 134*, 754-757. http://dx.doi.org/10.1016/j.jlumin.2012.06.052

Sakka, T., Masai, S., Fukami, K., & Ogata, Y. H. (2009). Spectral profile of atomic emission lines and effects of pulse duration on laser ablation in liquid. *Spectrochimica Acta Part B: Atomic Spectroscopy, 64*(10), 981-985. http://dx.doi.org/10.1016/j.sab.2009.07.018

Schmid, G. (1992). Large clusters and colloids. Metals in the embryonic state. *Chemical Reviews, 92*(8), 1709-1727. http://dx.doi.org/10.1016/j.apsusc.2005.07.150

Tarasenko, Vladimirovich, N., Butsen, A., Nevar, E., & Savastenko, N. (2006). Synthesis of nanosized particles during laser ablation of gold in water. *Applied surface science, 252*(13). http://dx.doi.org/4439-4444. 10.1016/j.apsusc.2005.07.150

Tarasenko, N., Butsen, A. & Nevar, E. (2005). Laser-induced modification of metal nanoparticles formed by laser ablation technique in liquids. *Applied surface science, 247*(1), 418-422. http://dx.doi.org/10.1016/j.apsusc.2005.01.093

Tolaymat, T. M., El Badawy, A. M., Genaidy, A., Scheckel, K. G., Luxton, T. P., & Suidan, M. (2010). An evidence-based environmental perspective of manufactured silver nanoparticle in syntheses and applications: a systematic review and critical appraisal of peer-reviewed scientific papers. *Science of the Total Environment, 408*(5), 999-1006. http://dx.doi.org/10.1016/j.scitotenv.2009.11.003

Tsuji, T., Iryo, K., Nishimura, Y., & Tsuji, M. (2001). Preparation of metal colloids by a laser ablation technique in solution: influence of laser wavelength on the ablation efficiency (II). *Journal of Photochemistry and Photobiology A: Chemistry, 145*(3), 201-207. http://dx.doi.org/10.1016/S1010-6030(01)00583-4

Tsuji, T., Iryo, K., Watanabe, N., & Tsuji, M. (2002). Preparation of silver nanoparticles by laser ablation in solution: Influence of laser wavelength on particle size. *Applied Surface Science, 202*(1), 80-85. http://dx.doi.org/ 10.1016/S0169-4332(02)00936-4

Tsuji, T., Thang, D. H., Okazaki, Y., Nakanishi, M., Tsuboi, Y., & Tsuji, M. (2008). Preparation of silver nanoparticles by laser ablation in polyvinylpyrrolidone solutions. *Applied Surface Science, 254*(16), 5224-5230. http://dx.doi.org/10.1016/j.apsusc.2008.02.048

Yang, G. (2012). Laser ablation in liquids: principles and applications in the preparation of nanomaterials: CRC Press.

Zhang, J. (2003). Self-assembled nanostructures (Vol. 2), Springer.